Epilepsy & Behavior Reports 27 (2024) 100676

Contents lists available at ScienceDirect

Epilepsy & Behavior Reports

journal homepage: www.elsevier.com/locate/ebcr

Delineating abnormal individual structural covariance brain network organization in pediatric epilepsy with unilateral resection of visual cortex

Liang Zhang [a,1], Bei Zhuang [c,1], Mengyuan Wang [b], Jie Zhu [a], Tao Chen [a], Yang Yang [a], Haoting Shi [a], Xiaoming Zhu [a,*], Li Ma [a,*]

[a] Department of Neurosurgery, Wuxi Clinical College of Anhui Medical University (The 904th Hospital of PLA), Wuxi, Jiangsu Province 214044, China
[b] Department of Nursing, Wuxi Clinical College of Anhui Medical University (The 904th Hospital of PLA), Wuxi, Jiangsu Province 214044, China
[c] Department of Anesthesiology, Wuxi Clinical College of Anhui Medical University (The 904th Hospital of PLA), Wuxi, Jiangsu Province 214044, China

ARTICLE INFO

Keywords:
Pediatric epilepsy
Individual
Structural covariance network
Graph-theory

ABSTRACT

Although several previous studies have used resting-state functional magnetic resonance imaging and diffusion tensor imaging to report topological changes in the brain in epilepsy, it remains unclear whether the individual structural covariance network (SCN) changes in epilepsy, especially in pediatric epilepsy with visual cortex resection but with normal functions. Herein, individual SCNs were mapped and analyzed for seven pediatric patients with epilepsy after surgery and 15 age-matched healthy controls. A whole-brain individual SCN was constructed based on an automated anatomical labeling template, and global and nodal network metrics were calculated for statistical analyses. Small-world properties were exhibited by pediatric patients after brain surgery and by healthy controls. After brain surgery, pediatric patients with epilepsy exhibited a higher shortest path length, lower global efficiency, and higher nodal efficiency in the cuneus than those in healthy controls. These results revealed that pediatric epilepsy after brain surgery, even with normal functions, showed altered topological organization of the individual SCNs, which revealed residual network topological abnormalities and may provide initial evidence for the underlying functional impairments in the brain of pediatric patients with epilepsy after surgery that can occur in the future.

Introduction

Epilepsy is a neurological disorder characterized by seizures that affect brain function [1]. Several studies have indicated structural and functional abnormalities in epilepsy [2–7]. However, an increasing number of studies have demonstrated that multiple brain regions frequently interact to form complex networks [8–14]. Graph theory was introduced to study the topological properties of the brain as a small world [15]. Small-world organization of the brain is important for functional integration and segregation [10]. Brain topographic abnormalities in epilepsy have been detected using electroencephalography, resting-state functional magnetic resonance imaging (MRI) and diffusion tensor imaging [16–18]. Surgical removal of epileptic lesions is one of the most important treatments. However, how the individual structural covariance network (SCN) topologically changes in epilepsy, especially in pediatric epilepsy after brain resection but with normal functions, remains unknown. Revealing residual network topological abnormalities in pediatric epilepsy after surgery could help in early intervention for functional decline.

Structural MRI offers an opportunity to noninvasively study brain morphology and coordinated developmental patterns in vivo [19–21]. Traditionally, brain networks have been mapped using functional MRI and diffusion MRI [22–27]. Structural MRI has many advantages over both functional and diffusion MRI, including ease of acquisition, high signal-to-noise ratio, and robustness to artifacts. A whole-brain structural network was proposed to explore the brain network topology by calculating inter-regional morphological similarities [28–30]. Previous studies have constructed SCNs at the group level by taking each individual subject as a time point, ignoring individual variability [29,31]. To characterize individual network topologies, Wang et al., [32] developed an individual morphological covariance network method to study abnormal network architectures in brain diseases [33,34]. An individual SCN may provide global insight into brain network topological organization patterns in pediatric epilepsy with resection of the visual cortex

* Corresponding authors.
E-mail addresses: zhuxiaoming_904@163.com (X. Zhu), mali_312@163.com (L. Ma).

[1] These authors contributed equally to this work.

https://doi.org/10.1016/j.ebr.2024.100676
Received 23 November 2023; Received in revised form 13 May 2024; Accepted 14 May 2024
Available online 16 May 2024

but with normal functions.

Herein, we used a noninvasive structural MRI technique and graph theory to map individual morphological covariance networks to investigate residual brain network topological abnormalities in seven pediatric patients with epilepsy after brain surgery and 15 age-matched healthy controls. From this new perspective, we aimed to reveal whether global brain network topological abnormalities exist in pediatric epilepsy after resection of epilepsy foci but with normal functions.

Material and methods

Participants

The structural MRI dataset of pediatric patients with epilepsy after surgery and healthy controls is a public dataset and was downloaded from the website https://kilthub.cmu.edu/articles/dataset/Pediatric_epilepsy_resection_MRI_dataset/9856205. Eight pediatric epilepsy patients with resection of epilepsy foci (six pediatric patients with resections to the ventral occipito-temporal cortex (VOTC) and two patients with resections outside the VOTC; mean age = 15.48 ± 2.83 years) and 15 age-matched healthy controls (3 female, 12 male, mean age = 14.5 ± 3.1 years) were included in this study (statistic p values: age, p = 0.67). The public dataset was collected at Carnegie Mellon University with data collection approved by the Institutional Review Boards of Carnegie Mellon University and the University of Pittsburgh [35]. Parents provided informed consent and minor participants were given assent prior to the scanning session [35]. The details for the subjects and dataset can be found in a previous study [35]. For all the eight pediatric epilepsy patients, one only provided structural T1 image before resection. Thus, only 7 participants with T1 images after resection were used for final analyses.

Structural MRI acquisition and preprocessing

Structural MRI data was acquired on a Siemens Verio 3T scanner with a 32-channel head coil at Carnegie Mellon University [35]. The imaging parameters for the structural MRI were as follows, repetition time (TR) = 2300 ms, echo time = 1.97 ms, acquisition time = 5m21s, voxel-wise resolution $1 \times 1 \times 1$ mm^3.

To map SCN, the structural MRI images were processed and the gray matter volume images were obtained using voxel-based morphology (VBM8) toolkit. The VBM analysis as follows: structural MRI images were first segmented into gray matter (GM), white matter (WM), and cerebrospinal fluid (CSF). The GM images were then transformed to Montreal Neurological Institute (MNI) space using Diffeomorphic Anatomical Registration using Exponentiated Lie algebra (DARTEL) approach. Finally, all the GM images were modulated and smoothed using a Gaussian kernel of 8 mm full-width at half maximum (FWHM) for further analyses [31,36].

Individual SCN analysis

Individual cortical SCN were calculated based on the automated anatomical labeling (AAL) template (including 90 cerebral regions) in both pediatric patients with epilepsy after surgery and healthy controls. Each subregion in AAL template was defined as a node and the edge of the individual SCN was defined as the inter-regional similarity of the distribution of the regional GM volume. To calculate the edge of the individual SCN, the kernel density estimation (KDE) was employed to estimate the probability density function of the extracted GM volume values of each AAL subregion and the variation of the KL divergence (KLD) is adopted to calculate the similarity between probability density functions. The similarities were taken as the edges of SCN [32,37], and a 90×90 correlation matrix for each subject was obtained for network analysis.

Network analyses

The binary network topology analyses were performed with the sparsity (S) of $0.05 < S < 0.4$ with step length of 0.02 [15,25]. Under each sparsity value, both global and nodal network parameters were calculated using graph theory with GRETNA software (http://www.nitrc.org/projects/gretna/). The network parameters included small-worldness, characteristic path length Lp, global efficiency E_{glob}, clustering coefficient C_p, local efficiency E_{loc}, synchronization, modularity, hierarchy, assortativity and two nodal centrality metrics: betweenness centrality B_e and degree K. For statistical analyses, the normalized value (area under the curve (AUC)) of the above parameters which is independent of single threshold selection was calculated. To identify the network parameters differences between pediatric epilepsy after surgery and healthy controls, Wilcoxon rank sum test was performed on the AUC of each network metric. The statistical results of the nodal parameters were corrected using false discovery rate (FDR) method with $p < 0.05$.

Results

Small-worldness of brain networks

Both the pediatric patients with epilepsy and healthy controls showed high gamma but almost identical lambda values compared with that in a random network ($\gamma \gg 1$ and $\lambda \approx 1$), indicating that the brain networks of pediatric patients with epilepsy after brain surgery and healthy controls were small-world organizations (Fig. 1).

Changed global network parameters in pediatric epilepsy

Graph theory was used to calculate individual SCN topological parameters to identify network topological changes in pediatric patients with epilepsy after brain surgery. Compared with healthy controls, pediatric patients with epilepsy exhibited significantly decreased global efficiency and increased shortest path length after brain surgery (Fig. 2). In addition, we compared other global parameters, including the clustering coefficient, local efficiency, degree, betweenness, synchronization, modularity, hierarchy, and assortativity, between patients with epilepsy after surgery and healthy controls, although no significant differences were found in these network topological parameters (Fig. 4).

Changed nodal network parameters in pediatric epilepsy

In addition to the global network parameters, we explored changes in the nodal network parameters in pediatric epilepsy after surgery. Compared with that in healthy controls, pediatric patients with epilepsy only showed a significantly increased nodal efficiency in the cuneus after brain surgery (Fig. 3). No other differences in other nodal parameters, such as betweenness, were observed.

Discussion

In this study, we used a novel individual SCN method to investigate topological differences between healthy controls and pediatric patients with epilepsy who underwent resection of the visual cortex but had normal functions. Three main findings were obtained. First, the SCN exhibited small-world properties in both healthy controls and pediatric patients with epilepsy after surgery, suggesting that the SCN is specifically suitable for investigating network reorganization in patients undergoing brain surgery. Second, pediatric patients with epilepsy after surgery showed reduced global efficiency but a higher shortest path length than healthy controls, indicating residual brain network abnormalities in pediatric patients with epilepsy after surgery, although no obvious functional impairments were observed. Third, pediatric patients with epilepsy showed increased nodal efficiency in the cuneus after surgery compared with that in healthy controls, suggesting functional

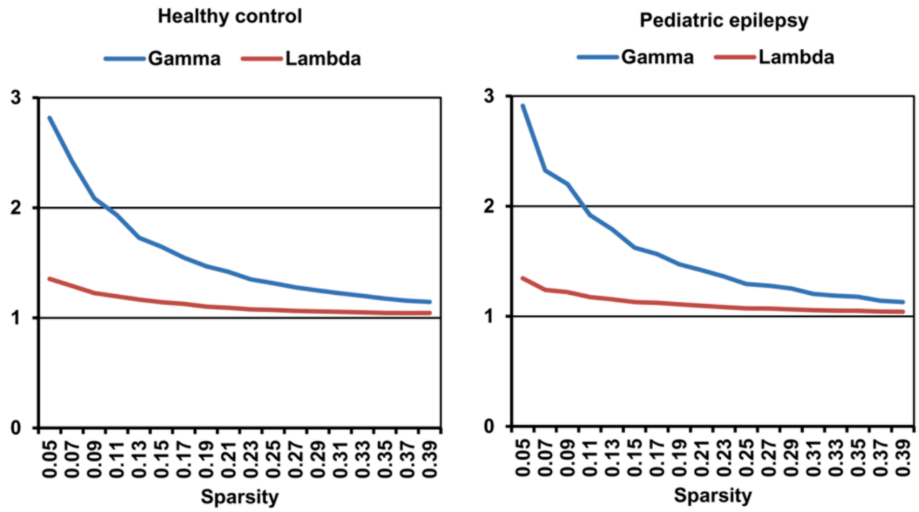

Fig. 1. The small-world attributes in pediatric patients with epilepsy after surgery and healthy controls. Under the sparsity from 0.05 to 0.4 with interval of 0.02, both pediatric patients with epilepsy and healthy controls showed small-world properties.

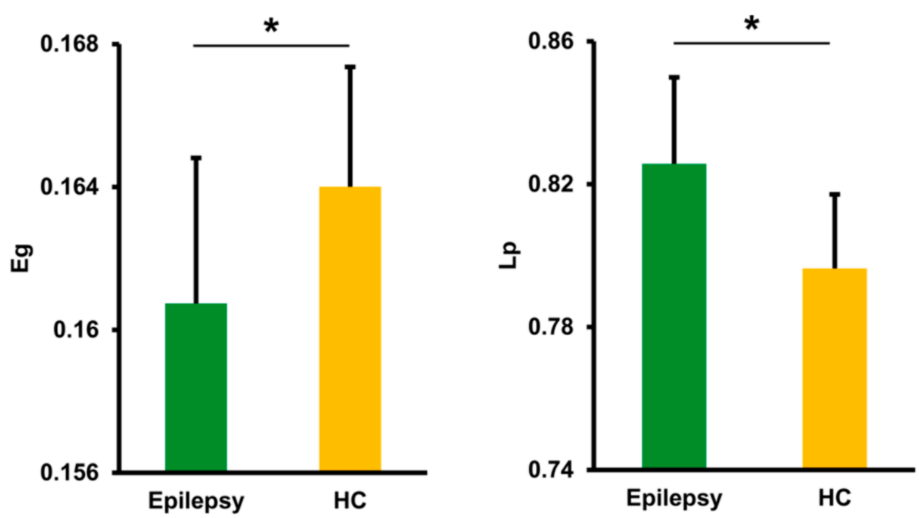

Fig. 2. Abnormal global network properties in pediatric patients with epilepsy after surgery. Pediatric patients with epilepsy after surgery showed decreased global efficiency while increased shortest path length compared to healthy controls.

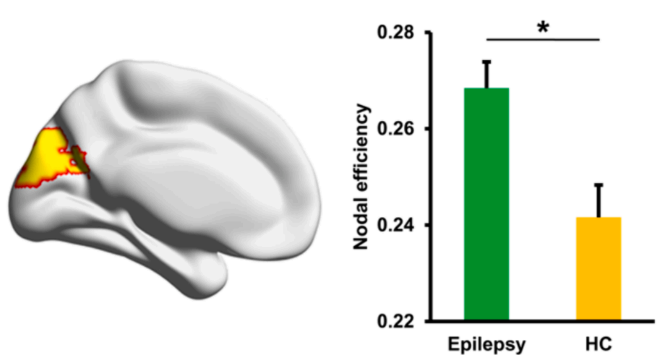

Fig. 3. Abnormal nodal efficiency in pediatric patients with epilepsy after surgery. Pediatric patients with epilepsy after surgery showed increased nodal efficiency of cuneus compared to healthy controls.

compensation of this area for visual cortex resection. In summary, these findings provide initial evidence for residual brain network topological abnormalities and functional compensation in pediatric epilepsy after visual cortex resection, which may provide insights into potential functional impairments occurring in the future.

The human brain is a complex system exhibiting small-worldness, functional segregation, and integration. [8]. We found that pediatric patients with epilepsy after brain surgery and healthy control subjects showed small-world topological properties of the SCN, consistent with previous findings obtained using other modalities [38]. The global topological properties of global efficiency and shortest path length changed significantly in pediatric patients with epilepsy after surgery compared with those in healthy controls. Our findings are supported by those of a previous group-level SCN study [39]. The global efficiency and shortest path length primarily reflect the network information transmission capabilities. The decreased global efficiency and increased shortest path length suggest that integration of global information was disrupted. Thus, although all pediatric patients with epilepsy showed normal function after brain surgery, the brain still had residual structural network topological abnormalities.

We also found that the local topological property of the nodal efficiency of the cuneus was significantly higher in pediatric patients with epilepsy after brain surgery than that in healthy controls. The cuneus plays an important role in processing visual information [40]. Given that

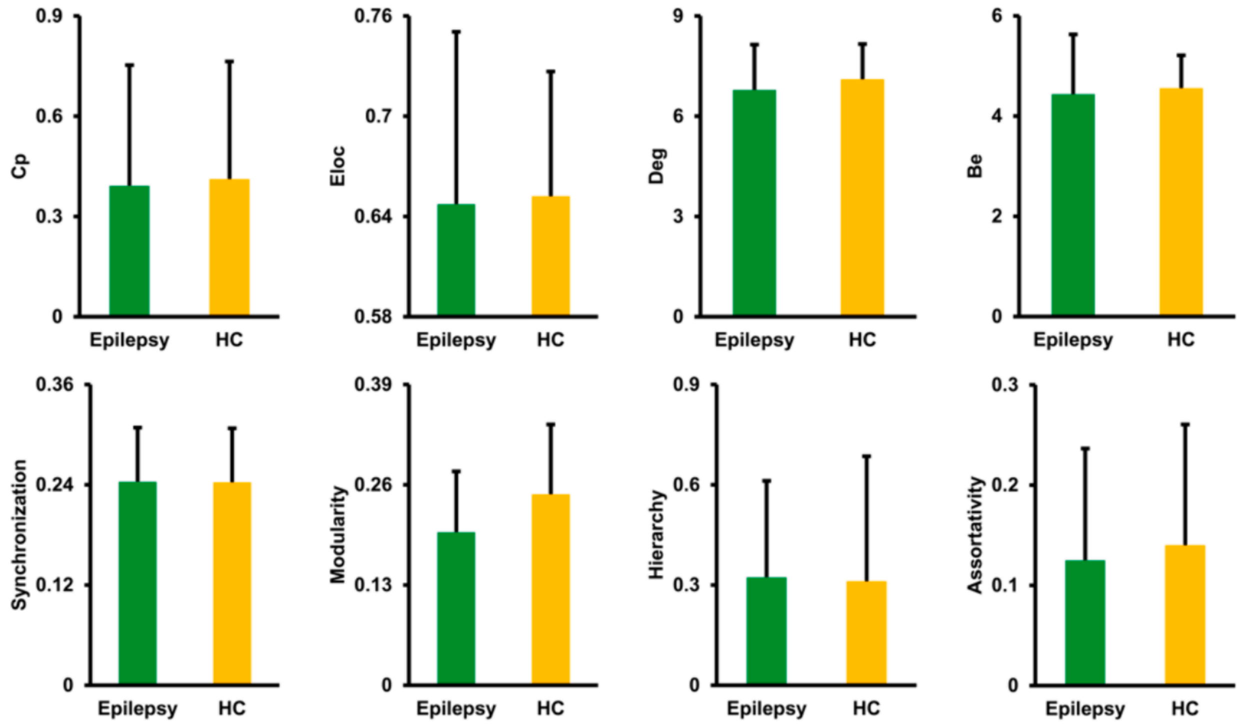

Fig. 4. The global network properties showing no significant differences in pediatric patients with epilepsy after surgery compared to healthy controls. There were no significant differences in network clustering coefficient (Cp), local efficiency (Eloc), degree (Deg), betweenness (Be), synchronization, modularity, hierarchy and assortativity in pediatric patients with epilepsy after surgery compared to healthy controls.

most pediatric patients with epilepsy have resections to the ventral occipitotemporal cortex but with normal functions, increased nodal efficiency of the cuneus suggests that these patients may have elevated visual information processing after surgery. Increased nodal efficiency may be a compensatory mechanism for damaged visual information-processing pathways in pediatric epilepsy after surgery. Overall, the increased nodal efficiency in the cuneus indicates that epilepsy after resection of the visual cortex may trigger the integration of visual information.

The current study has some limitations. First, although several previous studies have used a covariance approach to construct networks, the rationality of SCN must be validated compared with functional and anatomical network. Second, only seven pediatric patients with epilepsy after surgery were included in the current study, and the findings should be further validated in a larger sample. Third, this study used a public dataset that shared only MRI data and lacked other relevant information; however, given the uniqueness of the data, this study is noteworthy. Fourth, all patients with epilepsy underwent brain surgery, which may have affected the results of the brain network analysis. To avoid this problem, we employed an individual SCN method that uses the gray matter volume of voxels unaffected by surgery to obtain the distribution patterns of these matter volumes to calculate the regional similarity. This method can overcome the effects of brain surgery to a degree. Finally, sex information was not provided, and whether sex differences affect the results requires further study. Furthermore, the differences in the anatomical locations of brain resection may influence the results because of the small sample size.

Conclusions

We studied the individual SCN and graph theory in pediatric patients with epilepsy after surgery with no obvious functional impairments and revealed that these patients exhibited small-world properties after brain surgery. Compared with healthy controls, pediatric patients with epilepsy showed significantly decreased global efficiency, increased shortest path length, and increased nodal degree of the cuneus after surgery. These findings indicate that residual abnormalities of the brain network topological organization in pediatric patients with epilepsy with normal functions after resection of the visual cortex may help in the early prevention of potential functional impairments occurring in future.

Declarations

Ethics approval and consent to participate: All subjects gave informed written consent and the study protocols were approved by the Institutional Review Board of the Carnegie Mellon University and the University of Pittsburgh.

The structural MRI dataset of pediatric epilepsy patients and normal controls is a public dataset. The procedures used here were reviewed and approved by the Institutional Review Boards of Carnegie Mellon University and the University of Pittsburgh. Parents provided informed consent and minor participants gave assent prior to the scanning session.

Consent to publish: We have obtained consent to publish from the participant to report individual patient data.

Availability of data and materials: All the statistical data can be accessed by directly contacting the corresponding author.

Funding: Not applicable.

Authors' Contributions: L Ma, XM Zhu and L Zhang designed the experiment; L Zhang, B Zhuang, MY Wang, J Zhu, T Chen, Y Yang, and HT Shi collected and analysed the data, wrote and revised the paper; all the authors discussed the results.

CRediT authorship contribution statement

Liang Zhang: Writing – original draft, Formal analysis, Data curation. **Bei Zhuang:** Formal analysis, Data curation. **Mengyuan Wang:** Methodology, Formal analysis. **Jie Zhu:** Resources, Methodology. **Tao Chen:** Methodology. **Yang Yang:** Visualization, Validation. **Haoting Shi:** Visualization. **Xiaoming Zhu:** Writing – review & editing, Writing –

original draft, Supervision. **Li Ma:** Writing – review & editing, Supervision, Conceptualization.

Declaration of competing interest

The authors declare that they have no known competing financial interests or personal relationships that could have appeared to influence the work reported in this paper.

Acknowledgements

Not applicable.

References

[1] Kwan P, Brodie MJ. Early identification of refractory epilepsy. N Engl J Med 2000; 342(5):314–9. PubMed PMID: 10660394.
[2] Jiang S, Luo C, Liu Z, Hou C, Wang P, Dong L, et al. Altered local spontaneous brain activity in juvenile myoclonic epilepsy: A preliminary resting-state fMRI study. Neural Plast 2016;2016:3547203.
[3] Shaikh Z, Torres A, Takeoka M. Neuroimaging in pediatric epilepsy. Brain Sci. 2019;9(8):190. PubMed PMID: doi:10.3390/brainsci9080190.
[4] Fu C, Aisikaer A, Chen Z, Yu Q, Yin J, Yang W. Different functional network connectivity patterns in epilepsy: A rest-state fMRI study on mesial temporal lobe epilepsy and benign epilepsy with centrotemporal spike. Front Neurol. 2021;12. English.
[5] Alvim MKM, Coan AC, Campos BM, Yasuda CL, Oliveira MC, Morita ME, et al. Progression of gray matter atrophy in seizure-free patients with temporal lobe epilepsy. Epilepsia 2016;57(4):621–9.
[6] Iannetti P, Papetti L, Nicita F, Castronovo A, Ursitti F, Parisi P, et al. Developmental anomalies of the medial septal area: possible implication for limbic epileptogenesis. Childs Nerv Syst. 2011;27(5):765-70. PubMed PMID: 21057954. Epub 2010/11/09. eng.
[7] Spalice A, Nicita F, Papetti L, Ursitti F, Di Biasi C, Parisi P, et al. Usefulness of diffusion tensor imaging and fiber tractography in neurological and neurosurgical pediatric diseases. Childs Nerv Syst. 2010;26(8):995-1002. PubMed PMID: 20552206. Epub 2010/06/1eng.
[8] Sporns O, Tononi G, Kotter R. The human connectome: A structural description of the human brain. PLoS Comput Biol. 2005;1(4):e42. PubMed PMID: 16201007. Pubmed Central PMCID: 1239902.
[9] Bassett DS, Bullmore E. Small-world brain networks. The Neuroscientist 2006;12 (6):512–23. PubMed PMID: 17079517.
[10] Bullmore E, Sporns O. Complex brain networks: graph theoretical analysis of structural and functional systems. Nat Rev Neurosci 2009;10(3):186–98. PubMed PMID: 19190637.
[11] Wang J, Xie S, Guo X, Becker B, Fox PT, Eickhoff SB, et al. Correspondent functional topography of the human left inferior parietal lobule at rest and under task revealed using resting-state fMRI and coactivation based parcellation. Hum Brain Mapp 2017;38(3):1659–75. PubMed PMID: 28045222. Epub 2017/01/04. eng.
[12] Wang J, Yang Y, Fan L, Xu J, Li C, Liu Y, et al. Convergent functional architecture of the superior parietal lobule unraveled with multimodal neuroimaging approaches. Hum Brain Mapp. 2015;36(1):238-57. PubMed PMID: 25181023. Pubmed Central PMCID: 4268275.
[13] Yu X, Chen K, Ma Y, Bai T, Zhu S, Cai D, et al. Molecular basis underlying changes of brain entropy and functional connectivity in major depressive disorders after electroconvulsive therapy. CNS Neurosci Ther 2024;30(3):e14690.
[14] Chen K, Yang J, Li F, Chen J, Chen M, Shao H, et al. Molecular basis underlying default mode network functional abnormalities in postpartum depression with and without anxiety. Hum Brain Mapp. 2024;45(5):e26657. PubMed PMID: 38544486. Epub 2024/03/28.eng.
[15] Watts DJ, Strogatz SH. Collective dynamics of 'small-world' networks. Nature 1998;393(6684):440–2. PubMed PMID: 9623998.
[16] Chiang S, Haneef Z. Graph theory findings in the pathophysiology of temporal lobe epilepsy. Clin Neurophysiol. 2014;125(7):1295-305. PubMed PMID: 24831083. Pubmed Central PMCID: 4281254.
[17] Bernhardt BC, Chen Z, He Y, Evans AC, Bernasconi N. Graph-theoretical analysis reveals disrupted small-world organization of cortical thickness correlation networks in temporal lobe epilepsy. Cereb Cortex 2011;21(9):2147–57. PubMed PMID: 21330467.
[18] Vaessen MJ, Jansen JF, Vlooswijk MC, Hofman PA, Majoie HJ, Aldenkamp AP, et al. White matter network abnormalities are associated with cognitive decline in chronic epilepsy. Cereb Cortex 2012;22(9):2139–47. PubMed PMID: 22038907.
[19] Symms M, Jäger HR, Schmierer K, Yousry TA. A review of structural magnetic resonance neuroimaging. J Neurol Neurosurg Psychiatry 2004;75(9):1235–44.
[20] Wang J, Feng X, Wu J, Xie S, Li L, Xu L, et al. Alterations of gray matter volume and white matter integrity in maternal deprivation monkeys. Neuroscience 2018;1 (384):14–20. PubMed PMID: 29800718.
[21] Sun H, Sun Q, Li Y, Zhang J, Xing H, Wang J. Mapping individual structural covariance network in development brain with dynamic time warping. Cereb Cortex 2024;34(2):bhae039.
[22] Gong G, He Y, Concha L, Lebel C, Gross DW, Evans AC, et al. Mapping anatomical connectivity patterns of human cerebral cortex using in vivo diffusion tensor imaging tractography. Cereb Cortex. 2009;19(3):524-36. PubMed PMID: 18567609. Pubmed Central PMCID: 2722790.
[23] Gong G, Rosa-Neto P, Carbonell F, Chen ZJ, He Y, Evans AC. Age- and gender-related differences in the cortical anatomical network. J Neurosci. 2009;29(50): 15684-93. PubMed PMID: 20016083. Pubmed Central PMCID: 2831804.
[24] Hagmann P, Cammoun L, Gigandet X, Meuli R, Honey CJ, Wedeen VJ, et al. Mapping the structural core of human cerebral cortex. PLoS Biol. 2008;6(7):e159. PubMed PMID: 18597554. Pubmed Central PMCID: 2443193.
[25] Achard S, Bullmore E. Efficiency and cost of economical brain functional networks. PLoS Comput Biol. 2007;3(2):e17. PubMed PMID: 17274684. Pubmed Central PMCID: 1794324.
[26] Wang J, Wang Z, Zhang H, Feng S, Lu Y, Wang S, et al. White matter structural and network topological changes underlying the behavioral phenotype of MECP2 mutant monkeys. Cereb Cortex 2021.
[27] Wang J, Zuo Z, Xie S, Miao Y, Ma Y, Zhao X, et al. Parcellation of macaque cortex with anatomical connectivity profiles. Brain Topogr 2018;31(2):161–73. PubMed PMID: 28707157.
[28] Zhang Y, Lin L, Lin CP, Zhou Y, Chou KH, Lo CY, et al. Abnormal topological organization of structural brain networks in schizophrenia. Schizophr Res 2012; 141(2–3):109–18. PubMed PMID: 22981811. Epub 2012/09/18. eng.
[29] He Y, Chen ZJ, Evans AC. Small-world anatomical networks in the human brain revealed by cortical thickness from MRI. Cereb Cortex 2007;17(10):2407–19. PubMed PMID: 17204824.
[30] Bassett DS, Bullmore E, Verchinski BA, Mattay VS, Weinberger DR, Meyer-Lindenberg A. Hierarchical organization of human cortical networks in health and schizophrenia. J Neurosci. 2008;28(37):9239-48. PubMed PMID: 18784304. Pubmed Central PMCID: 2878961.
[31] Wu H, Sun H, Wang C, Yu L, Li Y, Peng H, et al. Abnormalities in the structural covariance of emotion regulation networks in major depressive disorder. J Psychiatr Res 2017;84:237–42. PubMed PMID: 27770743.
[32] Wang H, Jin X, Zhang Y, Wang J. Single-subject morphological brain networks: connectivity mapping, topological characterization and test–retest reliability. Brain Behav 2016;6(4):e00448.
[33] Gao J, Chen M, Li Y, Gao Y, Li Y, Cai S, et al. Multisite autism spectrum disorder classification using convolutional neural network classifier and individual morphological brain networks. Front Neurosci. 2021;14:629630-. PubMed PMID: 33584183. eng.
[34] Li X, Lei D, Niu R, Li L, Suo X, Li W, et al. Disruption of gray matter morphological networks in patients with paroxysmal kinesigenic dyskinesia. Hum Brain Mapp. 2021;42(2):398-411. PubMed PMID: 33058379. Epub 10/15. eng.
[35] Maallo AMS, Freud E, Liu TT, Patterson C, Behrmann M. Effects of unilateral cortical resection of the visual cortex on bilateral human white matter. Neuroimage 2020;207:116345.
[36] Wang J, Wei Q, Bai T, Zhou X, Sun H, Becker B, et al. Electroconvulsive therapy selectively enhanced feedforward connectivity from fusiform face area to amygdala in major depressive disorder. Soc Cogn Affect Neurosci. 2017;12(12):1983-92. PubMed PMID: 28981882. Pubmed Central PMCID: 5716231.
[37] Shen D, Li Q, Liu J, Liao Y, Li Y, Gong Q, et al. The deficits of individual morphological covariance network architecture in schizophrenia patients with and without violence. Front Psychiatry. 2021;12. English.
[38] Achard S, Salvador R, Whitcher B, Suckling J, Bullmore E. A resilient, low-frequency, small-world human brain functional network with highly connected association cortical hubs. J Neurosci 2006;26(1):63–72. PubMed PMID: 16399673.
[39] Yasuda CL, Chen Z, Beltramini GC, Coan AC, Morita ME, Kubota B, et al. Aberrant topological patterns of brain structural network in temporal lobe epilepsy. Epilepsia 2015;56(12):1992–2002. PubMed PMID: 26530395.
[40] Fan L, Wang J, Zhang Y, Han W, Yu C, Jiang T. Connectivity-based parcellation of the human temporal pole using diffusion tensor imaging. Cereb Cortex 2014;24 (12):3365–78. PubMed PMID: 23926116.